Renewable Energy 45 (2012) 59–71

Contents lists available at SciVerse ScienceDirect

Renewable Energy

journal homepage: www.elsevier.com/locate/renene

Implementing an effective finite difference formulation for borehole heat exchangers into a heat and mass transport code

Darius Mottaghy [a,*], Lydia Dijkshoorn [b,1]

[a] Geophysica Beratungsgesellschaft mbH, Lütticherstr. 32, D-52064 Aachen, Germany
[b] Institute for Applied Geophysics and Geothermal Energy, E.ON Energy Research Center, RWTH Aachen University, Mathieustr. 6, 52056 Aachen, Germany

ARTICLE INFO

Article history:
Received 10 December 2010
Accepted 5 February 2012
Available online 15 March 2012

Keywords:
Heat transport
Finite differences
Borehole heat exchanger

ABSTRACT

We present an effective finite difference formulation for implementing and modeling multiple borehole heat exchangers (BHE) in the general 3-D coupled heat and flow transport code SHEMAT. The BHE with arbitrary length can be either coaxial or double U-shaped. It is particularly suitable for modeling deep BHEs which contain varying pipe diameters and materials.

Usually, in numerical simulations, a fine discretization of the BHE assemblage is required, due to the large geometric aspect ratios involved. This yields large models and long simulation times. The approach avoids this problem by considering heat transport between fluid and the soil through pipes and grout via thermal resistances. Therefore, the simulation time can be significantly reduced.

The coupling with SHEMAT is realized by introducing an effective heat generation. Due to this connection, it is possible to consider heterogeneous geological models, as well as the influence of groundwater flow. This is particularly interesting when studying the long term behavior of a single BHE or a BHE field. Heating and cooling loads can enter the model with an arbitrary interval, e.g. from hourly to monthly values. When dealing with large BHE fields, computing times can be further significantly reduced by focusing on the temperature field around the BHEs, without explicitly modeling inlet and outlet temperatures. This allows to determine the possible migration of cold and warm plumes due to groundwater flow, which is of particular importance in urban areas with a high BHE installation density.

The model is validated against the existing BHE modeling codes EWS and EED. A comparison with monitoring data from a deep BHE in Switzerland shows a good agreement. Synthetic examples demonstrate the field of application of this model.

1. Introduction

Ground source heat pump systems (GSHP) using borehole heat exchangers (BHE) as an energy source are becoming more and more popular due to the increase in prices for fossil energy and low running costs. Furthermore, the infinite energy stock of geothermal energy at timescales of mankind makes this source a renewable one. Whereas single or multiple shallow BHEs (<200 m) are used for heating residential and commercial buildings together with a heat pump, deep BHEs (up several km) produce temperatures high enough for direct use, heating several buildings and even whole districts, depending on depth, diameter, and flow rate.

A BHE consists of a closed loop or coaxial pipes lowered into a borehole. Whereas the first layout is widely used in the field of shallow geothermal energy, the latter one is mostly applied to deep BHE installations. Grout is used to fill up the void between borehole wall and pipes, ensuring a good thermal contact on the one hand, and a sealing on the other hand. The circulating fluid can be water or some mixture of water and antifreeze. It is cooled within a heat pump which transfers the extracted energy to desired temperature levels. Fig. 1 shows a schematic sketch of a shallow BHE installation. Shallow BHEs can also be run in “reverse” mode for cooling. A review of different kinds of ground heat exchangers is given in Florides and Kalogirou [1].

The comparatively high investment costs for construction require a thorough planning of the system, regarding both the desired heating and cooling loads, as well as the geological situation. Since these installations are intended for a long life cycle, it is important to predict their behavior for several decades.

There are different numerical tools regarding the modeling of system performance of borehole heat exchangers, e.g. the Earth

* Corresponding author.
E-mail addresses: d.mottaghy@geophysica.de (D. Mottaghy), lydia.dijkshoorn@agentschapnl.nl (L. Dijkshoorn).
[1] Present address: Divisie NL Energie en Klimaat, Agentschap NL, Sittard, The Netherlands

0960-1481/$ – see front matter © 2012 Elsevier Ltd. All rights reserved.
doi:10.1016/j.renene.2012.02.013

Nomenclature

t	time, s
r	radius, m
A	area, m^2
V	volume, m^3
υ	velocity, m s^{-1}
λ	thermal conductivity, W m^{-1} K^{-1}
ν	kinematic viscosity, m^2 s^{-1}
ρ	mass density, kg m^{-3}
c_p	specific heat capacity, J kg^{-1} K^{-1}
$C = \rho\, c_p$	volumetric heat capacity, J m^{-3} K^{-1}
Q	thermal energy, J
$\dot{Q} = dQ/dt$	heat flow rate, J s^{-1}
h	heat transfer coefficient, W m^{-2} K^{-1}
T	temperature, °C
R	thermal resistance, K W^{-1}
F	fluid flow rate inside borehole heat exchanger, m^3 s^{-1}
Bu	Shank space (double-U), m

Numbers

Nu	Nusselt number
Pr	Prandtl number
Re	Reynolds number

Subscripts

b	borehole
w	parameter of the water
r	parameter of the rock
gr	parameter of the grout
e	effective mean parameter
inner	inner pipe (coaxial)
outer	outer pipe (coaxial)
pipe	pipe (Double-U)

Energy Designer [2], or the code EWS described in [3]. A realistic prediction of the long term behavior helps to design the BHE according to the desired requirements. The aforementioned codes are fast, since they use rotational symmetry and are completely or partly based on analytical solutions, the so called g-functions [4]. However, the restriction to rotational symmetry does not allow taking into account the influence of groundwater flow which can affect the subsurface heat transport significantly. Furthermore, the representation of the geologic conditions is restricted to homogeneous or layered media. Only a few studies like Diao et al. [5] and Sutton et al. [6] include heat advection by groundwater flow in their modeling approaches, based on pure analytical solutions. In order to consider an arbitrary geological situation, a numerical 3-D model is necessary. These direct numerical solutions, e.g. finite difference, finite volume, finite element [7–10] are or have been used to model borehole heat exchangers. However, this in turn yields new problems, because the complex geometrical configuration of the exchangers make the numerical analysis complicated and computationally very demanding. The reason are the extreme aspect ratios of BHE systems, e.g. the ratio between pipe diameter/thickness and length, associated with various thermodynamic interactions on different time scales occurring between the fluid flow in the pipes, the pipe assemblage itself, the borehole, and the surrounding geological media. Therefore, a grid or mesh with sufficient resolution must be set up in order to account for all these processes and to obtain a stable numerical solution. This results in long computing times, depending on the time periods to be simulated.

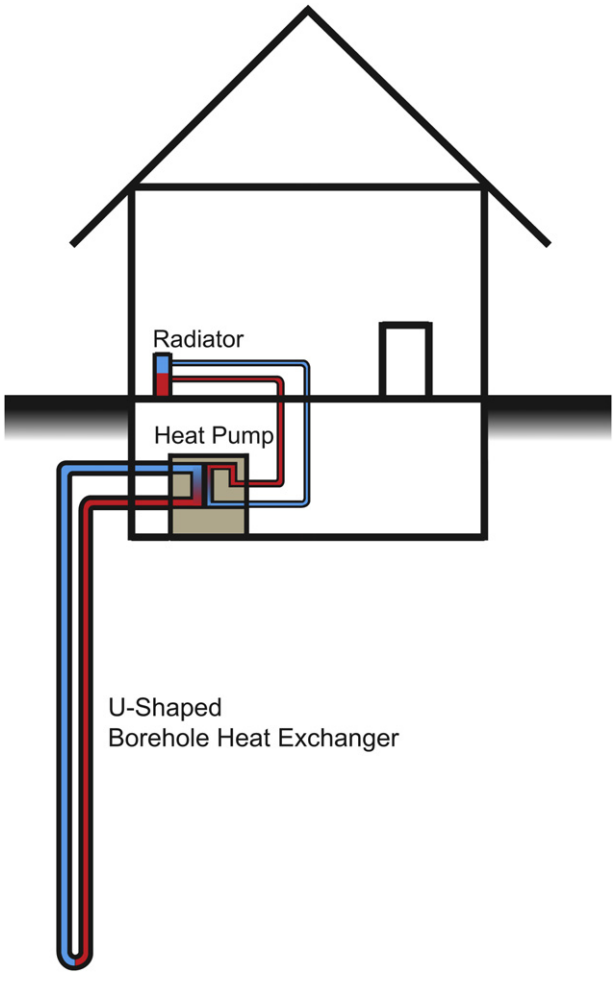

Fig. 1. Sketch of a shallow BHE installation for domestic use. Heat is extracted from the underground by a heat pump with a closed U-shaped loop as a heat exchanger.

Thus, it is important to develop numerical strategies to reduce computing times without any restrictions for the BHE itself and the surroundings, and which keep the possibility of arbitrary boundary conditions.

In this paper, we present an approach which veers toward these desired properties. It comprises the coupling of a Finite Difference (FD) approach for calculating heat transfer processes within the BHE and a general heat and transport code. Therefore, our approach can be considered as situated between entirely numerical and purely analytical methods. Consequently, it allows to account for all features which direct numerical methods include, but using less computing power. Regarding advective conditions, as well as geological more complicated situations, it is often important to study the long term behavior and to perform sensitivity studies in order to find a proper design for the BHE system. The reasons are the long time periods which are possibly necessary until the system shows a balanced thermal situation, that is a steady-state condition.

Our approach utilizes the fact that the typical BHE geometry changes in radial direction, but is rather constant in vertical direction. Thus, in order to avoid the very fine radial discretization,

thermal resistances are used to compute heat transfer horizontally, whereas finite differences are used in the vertical direction. The concept of thermal resistance in the field of BHE modeling is used in different modeling tools, such as those mentioned above, and discussed by several authors. Lamarche et al. [11] present an overview and comparison of different approaches regarding the determination of borehole and internal thermal resistances of a single U-shaped BHE. Others developed models of BHEs for the use in existing energy system modeling tools [12], or as a stand-alone tool [13]. In our work, we use the concept of thermal resistances and its application to cylindrical components as described in Çengel et al. [14].

Originally, our study started with applying the thermal resistance method to the modeling of a deep BHE, which was intended to be placed in the 2.5 km deep borehole RWTH-1 in Aachen, Germany, at that time [15–17]. Whereas the concept of using thermal resistances is not new, the coupling of all processes in a coaxial BHE with varying pipe assemblages, taking into account upward and downward flow, was a novel approach by that time. In fact, De Carli et al. [13] also study coaxial pipes in a similar way regarding the resistances, but restricted to one pipe diameter and using radial symmetry.

Dijkshoorn [18] extensively describes an analytical approach for modeling this process for a homogeneous rocks with a linear geothermal gradient and a constant borehole heat exchanger geometry with depth. Dijkshoorn [18] also presents a semi-analytical FD formulation in order to consider layers of different rocks, a non linear behavior of the thermal gradient, and a changing geometry of the borehole heat exchanger with depth. However, the study of Dijkshoorn [18] restricts to coaxial BHEs. Here, we enhance the approach by U-shaped BHEs, which are commonly used in shallow geothermal installations.

After some modifications, this approach is implemented in the FD code SHEMAT [19]. This very general code solves coupled problems involving fluid flow, heat and mass transport on an FD grid. It can be also applied to studies in cold regions or freezing problems since it considers phase change effects such as latent heat and permeability decrease. Additionally, it can handle chemical water–rock interactions. Therefore, it can be utilized for a variety of thermal and hydrogeological problems (see Fig. 2). This implementation allows to set up arbitrary geological models with SHEMAT, in which the BHE models can be placed. SHEMAT also considers the temperature and pressure dependence of thermal and hydraulic properties, which becomes particularly important for deep BHEs, where larger variations of ground temperatures prevail. SHEMAT, like many other codes, does not take the hydrodynamic component of thermal dispersion into account, however, this is justified since thermal diffusion is more efficient than molecular diffusion by several orders of magnitude [20]. Nevertheless, the effect of macrodispersion due to heterogeneity at larger scales may have an influence on the thermal field (e.g. [21]), which can be important when dealing with simulations of injection and production from geothermal reservoirs. For shallow systems, the issue about thermal dispersion is also currently studied, Molina-Giraldo et al. [22] for instance find a possible influence of thermal dispersion on temperature plumes around a BHE, depending on the subsurface type. In our examples about the influence of groundwater flow on BHE systems, we show the principal processes and thus restrict to coupled heat and flow modeling without considering thermal dispersion.

The possibility of considering varying pipe diameters and borehole assemblages makes our method particulary suitable for deep BHEs. In this case, groundwater flow usually does not have a significant influence so that cylindrical models can be invoked, provided there is a layered structure of the subsurface. This reduces computing times considerably. Fig. 3 shows the situation for this kind of a deep, coaxial BHE. It consists of an outer pipe where the fluid moves downwards, gradually warming. The heated water rises in the inner pipe, which is then used by the heat pump. The sketch also indicates the change of the assemblage due to the different

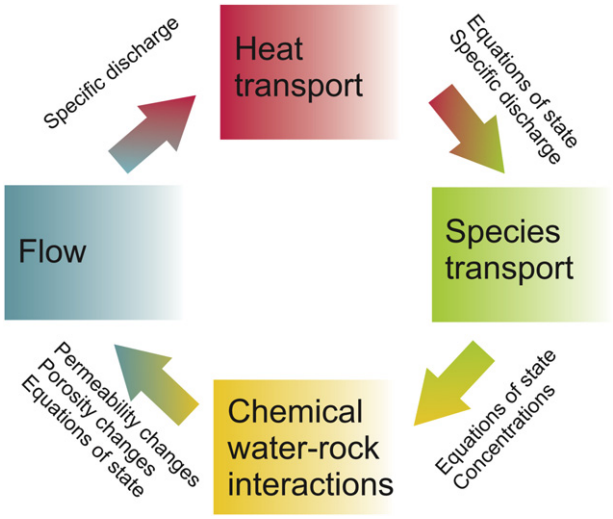

Fig. 2. Overview of the different processes which can be simulated with the code SHEMAT.

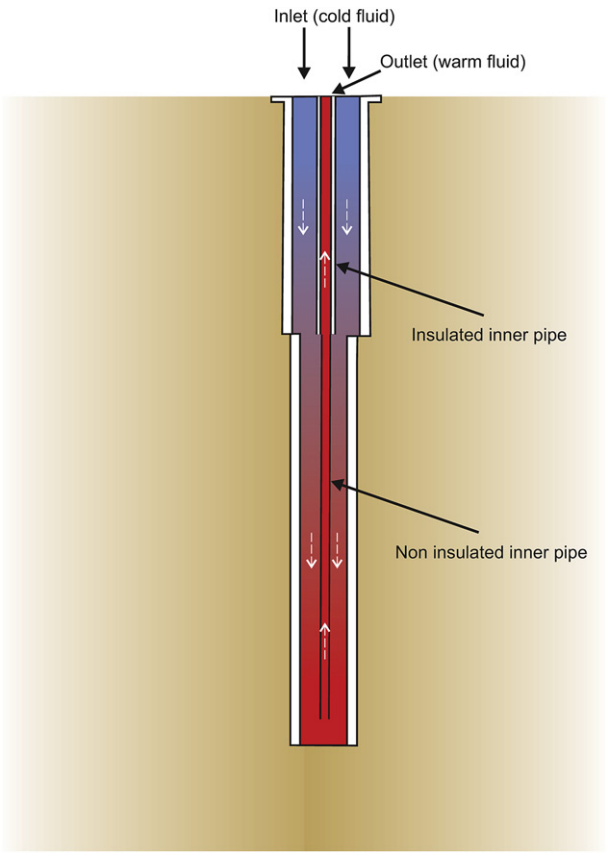

Fig. 3. Sketch of a deep BHE with varying pipe assemblages. Cool water moves downward in the outer pipe, warming up with increasing depth. The warm water is pumped up in the inner pipe.

packers in the borehole. From there downwards, the inner pipe changes from insulated to non-insulated configuration. This is justified since the temperature of the downward moving water is high enough not to significantly cool the warm water rising in the inner pipe. Monitoring data from such kind of deep BHE is used for validation of our BHE model approach (see Section 3).

Although our approach saves computing resources in comparison to pure numerical modeling, it has restrictions when dealing with large BHE fields: The requirements for computing power become too high and processing times would be too long. Regarding these cases, we developed a simplified version of our approach, which does not explicitly calculate the inlet and outlet temperatures of the BHEs; it restricts the model to simulating the impact of the BHE field on the temperature regime in the subsurface, based on the SHEMAT code itself. However, this still allows characterizing hot and cold plumes in terms of their temporal and spatial development. This is an important issue, in particular in densely populated areas (see Section 4).

As a conclusion, we suggest some combined procedure for designing BHE fields, which depends on the different geological and technical conditions (see Section 5).

2. Semi-analytical FD formulation for the coaxial BHE

The FD formulation of the presented approach involves the determination of thermal resistances of the different parts of the BHE, it is described in the following.

The coaxial BHE is divided into grid cells with vertical dimension $dz = v_w^{inner} dt$, where dt is the time step, and v_w^{inner} the fluid velocity in the inner pipe, which is $v_w^{inner} = F_w/(\pi r_{inner}^2)$, with the flow rate F_w and the radius of the inner pipe r_{inner}^2 (see Fig. 4). It does not require the fine radial discretization of a BHE since it considers heat transport between the inner hot pipe and the outer cold pipe as well as heat transport between the outer cold pipe and the soil as thermal resistances (e.g. [14]).

The properties of the grid cells representing the pipe are defined at the center of the cells, and the temperatures of the inner and outer pipe are defined at the top and bottom of the cells. Temperatures of the underground are also defined at the center of the cells.

The formulation consists of two stacks of grid cells; one in the cold outer pipe and one in the hot inner pipe. They are analytically connected with each other by the cylindrical heat balance equation.

Considering the energy balance equation, we define the total heat flow rate $\dot{Q}$ going into and out of each grid layer i. For this, we distinguish between two different situations; the *flow case* where the water inside the borehole heat exchanger circulates and the *no-flow case*, where the water does not circulate.

In case of the active BHE with fluid circulating (*flow case*, Fig. 4), taking the energy balance into account, we get

$$T_d^t(i+1) = \frac{-\dot{Q}_e + \dot{Q}_r}{C_w F_w} + T_d^{t-1}(i) \tag{1}$$

$$T_u^t(i) = \frac{\dot{Q}_e}{C_w F_w} + T_u^{t-1}(i+1) \tag{2}$$

with

$$\dot{Q}_e = \frac{\left(T_d^{t-1}(i+1) + T_d^{t-1}(i)\right)}{2} - \frac{\left(T_u^{t-1}(i+1) + T_u^{t-1}(i)\right)}{2} \Big/ R_{inner} \tag{3}$$

$$\dot{Q}_r = T_r^{t-1} - \frac{\left(T_d^{t-1}(i+1) + T_d^{t-1}(i)\right)}{2} \Big/ R_{outer} \tag{4}$$

where $\dot{Q}_e$ is the heat flow rate between the inner and outer pipe, $\dot{Q}_r$ the heat flow rate from the rocks to the outer pipe, and T_u and T_d the temperature of the inner and outer pipe, respectively. The superscript $(t-1)$ indicates the index of the previous time step, $(i+1)$ indicates the index of the grid layer, R the thermal resistance defined in the Appendix and C_w the volumetric heat capacity of the fluid. In the flow case, the vertical heat transport is dominated by advection, thus we neglect the vertical conductive heat flow in the

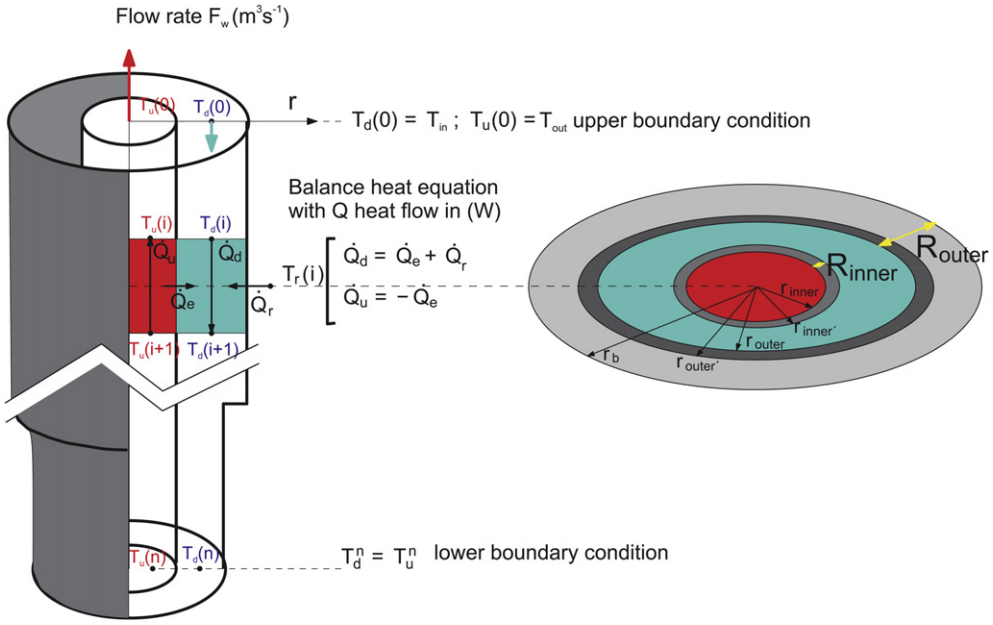

Fig. 4. A schematic figure of a running BHE (*flow case*) with heat energy balance equations.

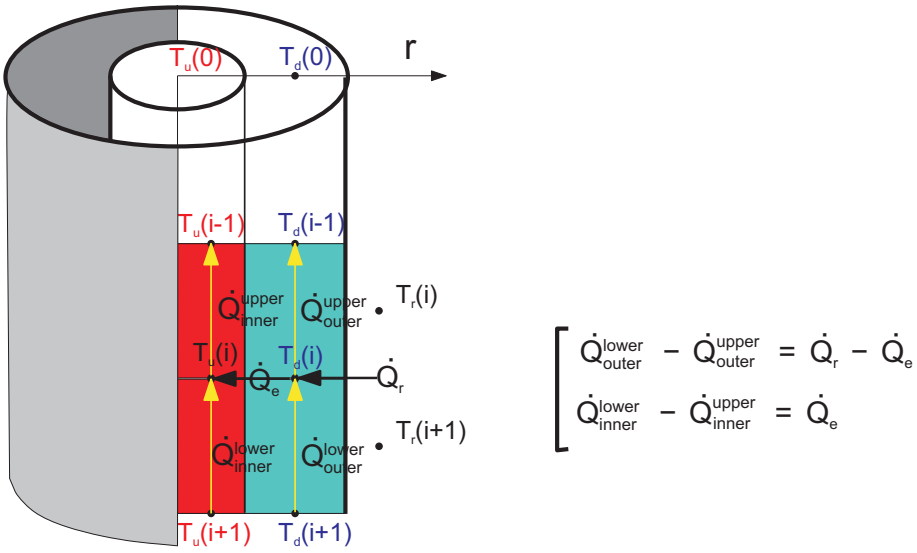

Fig. 5. A schematic figure of a borehole heat exchanger with heat energy balance equations in case of no fluid circulation, a passive BHE.

fluid which has a low thermal conductivity. The derivation of R_{outer} and R_{inner} is described in Appendix A.1 and Appendix A.2.

In case of the passive BHE (*no flow*, Fig. 5), the energy balance yields:

$$T_d^t = T_d^{t-1} + \frac{\mathrm{d}t}{\mathrm{d}zA_{outer}C_w}\left(-\dot{Q}_e + \dot{Q}_r - \dot{Q}_{outer}^{upper} + \dot{Q}_{outer}^{lower}\right) \quad (5)$$

$$T_u^t = T_u^{t-1} + \frac{\mathrm{d}t}{\mathrm{d}zA_{inner}C_w}\left(\dot{Q}_e - \dot{Q}_{inner}^{upper} + \dot{Q}_{inner}^{lower}\right) \quad (6)$$

with

$$\dot{Q}_{inner}^{upper} = \frac{T_u^{t-1}(i+1) - T_u^{t-1}(i)}{R_u} \quad (7)$$

$$\dot{Q}_{inner}^{down} = \frac{T_u^{t-1}(i) - T_u^{t-1}(i-1)}{R_u} \quad (8)$$

$$\dot{Q}_{outer}^{upper} = \frac{T_d^{t-1}(i+1) - T_d^{t-1}(i)}{R_d} \quad (9)$$

$$\dot{Q}_{outer}^{down} = \frac{T_d^{t-1}(i) - T_d^{t-1}(i-1)}{R_d} \quad (10)$$

$$\dot{Q}_e = \frac{T_d^{t-1}(i) - T_u^{t-1}(i)}{R_{inner}} \quad (11)$$

$$\dot{Q}_r = \frac{\left(T_r^{t-1}(i+1) + T_r^{t-1}(i)\right)}{2} - T_d^{t-1}(i) \quad (12)$$

with the volumetric heat capacity C_w and R_u, R_d, R_{inner} and R_{outer} the resistances of water in the inner and outer pipe, respectively, and the resistances through the inner and outer pipe as described in Appendix A.1 and Appendix A.2. A_{outer} and A_{inner} denotes the outer and inner flown through area of the pipes.

2.1. Formulation for the double U-shaped BHE

For the double U-shaped BHEs, a similar approach as above is used. However, because of the more complex geometry of this kind of BHE (see Fig. 6), the determination of thermal resistances is not trivial. More parameters like the shank space *Bu* in Fig. 6 must be taken into account, and there is not such a radial symmetry as for the coaxial BHE. Hellström [23] gives an extensive derivation of the thermal resistances R_a and R_b which we use here (see Appendix A.4). R_a is the internal thermal resistance used for calculating the heat flow rates analogous to equation (3) and R_b the borehole resistance from which the heat transfer to SHEMAT is computed, analogous to equation (4). Furthermore, different fluid properties must be taken into account since the working fluids are usually not pure water, but contain some part of antifreeze agent.

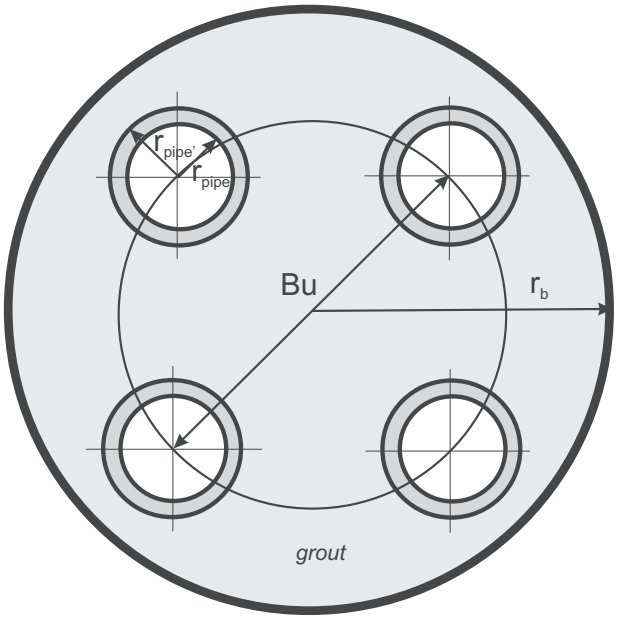

Fig. 6. Cross section of a double-U shaped BHE with the characteristic geometric properties.

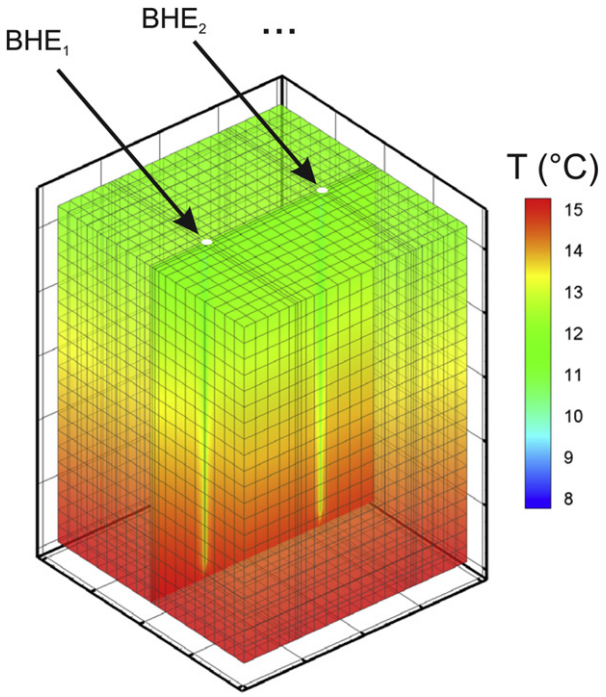

Fig. 7. Temperature distribution around two running BHEs which are extracting heat. A BHE is placed anywhere in a 3-D model, defined by the i*th* and j*th* node in the finite difference grid.

2.2. The coupling with SHEMAT

The coupling with the heat and fluid transport code SHEMAT is realized by introducing an effective heat generation which results from the heat flow rate to or from the outer pipe $\dot{Q}_r$. In turn, the underground temperature T_r calculated from SHEMAT enters the BHE model.

Due to this connection, it is possible to consider an arbitrary, heterogenous geologic model, as well as the influence of groundwater flow. Fig. 7 illustrates the placement of one or several BHE in a 3-D SHEMAT model.

The inlet temperature or the power, and the pump rate can be chosen according to individual requirements. The numerical simulations show that the additional computing time needed for modeling the developed BHE module is negligible. However, the time steps must be kept comparatively small, in order to fully account for the flow within the pipes, and to meet the numerical requirements such as the Courant criterion (e.g. [24]).

On the one hand the number of grid nodes can be much smaller than in pure numerical models, on the other hand the time step sizes must not exceed a particular value. This means that it is possible to model one or a few BHEs, but not a whole BHE field. In this case one or few representative BHE can be regarded, studying the influence of groundwater flow on outlet temperatures and power.

However, often it is interesting to determine the influence on the subsurface temperatures of a running BHE field in the long term, and the explicit calculation of inlet and outlet temperatures is subordinate. This inspired us to develop a simplified version of this approach without explicitly simulating inlet and outlet temperatures. It rather calculates the thermal impact on the subsurface of the BHEs when providing heating and cooling loads (see section 4).

In the case of deep BHEs however, there is usually one system to be studied. Hence, the explicit approach is particularly adapted for these kind of BHEs, not least because the vertical disctretization allows to consider the varying diameters of deep borehole assemblages.

Table 1
Required input parameters for the BHE simulations.

BHE geometry	
U-Shape	Borehole diameter, length, Pipe diameters, shank space
Coaxial	Borehole diameter (varying), length Pipe diameters (varying)
BHE load profile	
Power or inlet temperature	Heat and cooling load (Monthly, daily, hourly, on-off times)
Thermal properties	Pipes, grout, fluid

Table 2
Properties of the BHE after [9].

Parameter	Value
Borehole diameter	0.115 m
Pipe diameter, thickness	32 mm, 2.9 mm
Pipe thermal conductivity	0.42 W m^{-1} K^{-1}
Length	100 m
Flow rate	1.476 m^3 h^{-1}
Fluid	Water-Ethylenglycole (20%)
Power (varying)	208 W–2070 W
Ground and grout thermal conductivity	2.46 and 0.81 W m^{-1} K^{-1}
Ground thermal capacity	2.6 MJ m^{-3} K^{-1}
Simulation time	1 year

2.3. Requirements for BHE simulations

The explicit simulation of BHE systems requires several input parameters to solve the heat balance calculations described above. They are listed in Table 1. The necessary load profiles must contain either the power, or the inlet temperature of the BHE within arbitrary time intervals, including rest intervals. The information about the BHE geometry such as length, varying borehole and pipe diameters, together with thermal data for each material and the fluid complete the data set on the BHE system.

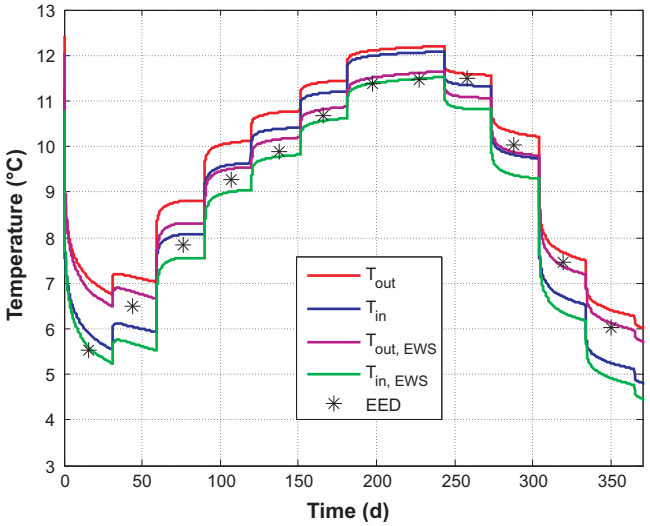

Fig. 8. Comparison of the modeled temperatures with the programs EED and EWS, the example is taken from in [9]. EED only calculates mean fluid temperatures.

Table 3
Monthly profile used in the simulation after [9].

Month	Runtime per month (h)	Energy load per month (kWh)
January	308	1540
February	252	1260
April	186	930
April	119	595
May	93	465
June	60	300
July	31	155
August	31	155
September	60	300
October	124	620
November	240	1200
December	296	1480
Total	1800	900

The subsurface model itself is set up in terms of the locations of the BHEs. In case of a single BHE and no significant groundwater flow, it is sufficient to build a model with cylindrical symmetry which saves computing resources. If ground water flow is present, or there is a complicated geology, a 3-D model is necessary. In either case, the grid must be refined at the BHE location, since the area of the regarded grid block must correspond to the cross sectional area of the borehole containing the BHE. Necessary CPU-times vary with the different set-ups. This is also generally the reason that it is not easy to compare CPU-times necessary for different software tools, only taking information from literature. Various parameters such as those of the model, the numerical procedure, and the hardware have an impact on computational times, thus, only a direct comparison with an identical model and hardware set up allows reliable statements. Therefore, we compare our new approach with a model using a fully numerical and discretized model in SHEMAT for a deep BHE, similar to the one in [16]. This allows us to give a quantitative statement on the reduction of CPU-times. For the model for code verification shown below, the CPU-time with the approach presented here is about an hour for one year simulation time, compared to two days for a model using a fully discretized model with SHEMAT alone.

3. Model validation and application

In order to validate the presented method, we compare it with other programs, as well as monitoring data from an existing deep BHE. Furthermore, we show the field of application by some synthetic examples, regarding the performance of a deep BHE, and the influence of groundwater flow on a shallow system.

3.1. Comparison with other software

The comparison with the existing programs EED [2] and EWS [3] features the simulation of a U-shaped BHE in a homogenous subsurface. The model for the BHE is taken from a study in [9]. In a next step, we use field data from a deep borehole to test our code.

In the first model, the thermal load of a standard BHE (Table 2) is varied according to an annual profile (Table 3). The program EED does not determine outlet and inlet temperatures explicitly, it rather computes a mean fluid temperature along the entire BHE as a monthly average, solving involved equations semi-analytically. This mean temperature can be regarded as the mean value between BHE outlet and inlet temperature, $(T_{out} + T_{in})/2$ [9].

Taking this into account, temperatures modeled with EED and with our approach are compared at the middle of each month (Fig. 8). The maximum deviation between both methods are approx. 0.5 K, which is a good agreement, since there are different modeling approaches, and EED only calculates a mean fluid temperature. The comparison with the results from the EWS program yields similar deviations. EWS uses different modeling methods for the near and far field. Whereas close ($\lesssim$3 m) to the BHE a numerical procedure with rotational symmetry is used, the processes farther away are solved by using g-functions.

Signorelli and Kohl [25] compare the EWS program with the software FRACTURE [26]. The latter one uses the Finite Element method and solves the problem purely numerically. Signorelli and Kohl [25] find a good agreement between both modeling programs, but also with systematic slightly higher temperatures for the FRACTURE model, but the difference remains less than 0.2 K in the long term behavior.

Besides the different modeling approaches used by EWS and our method, we found the fluid properties to play an important role in our case. Sensitivity studies show that the temperature dependence of thermal and hydraulic properties, as well as the volume fraction of the water-ethylene glycol mixture have a systematic influence on the simulated temperatures. This results in a systematic, slight offset between EWS and our method. In the model shown here, we use water as a fluid, and the systematic

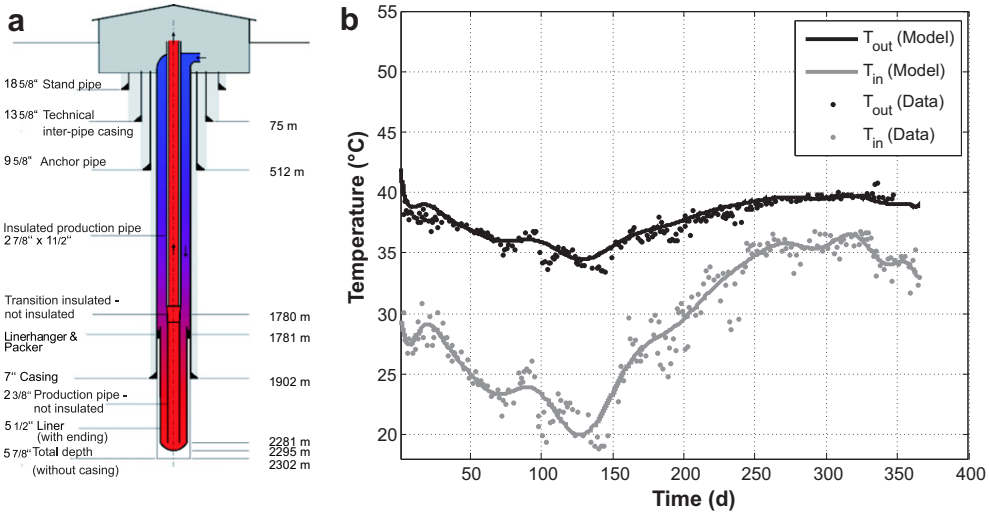

Fig. 9. (a) The deep BHE in Weggis, Switzerland (adapted from. [30]). (b) Comparison with monitoring data from the deep BHE in Weggis, Switzerland [27].

higher temperatures seem to result from the different water properties used, besides the generally different approach as described above.

In summary, we conclude that our approach produces reasonable results. The deviations are in the same order of magnitude as between the other two programs themselves, EWS and EED.

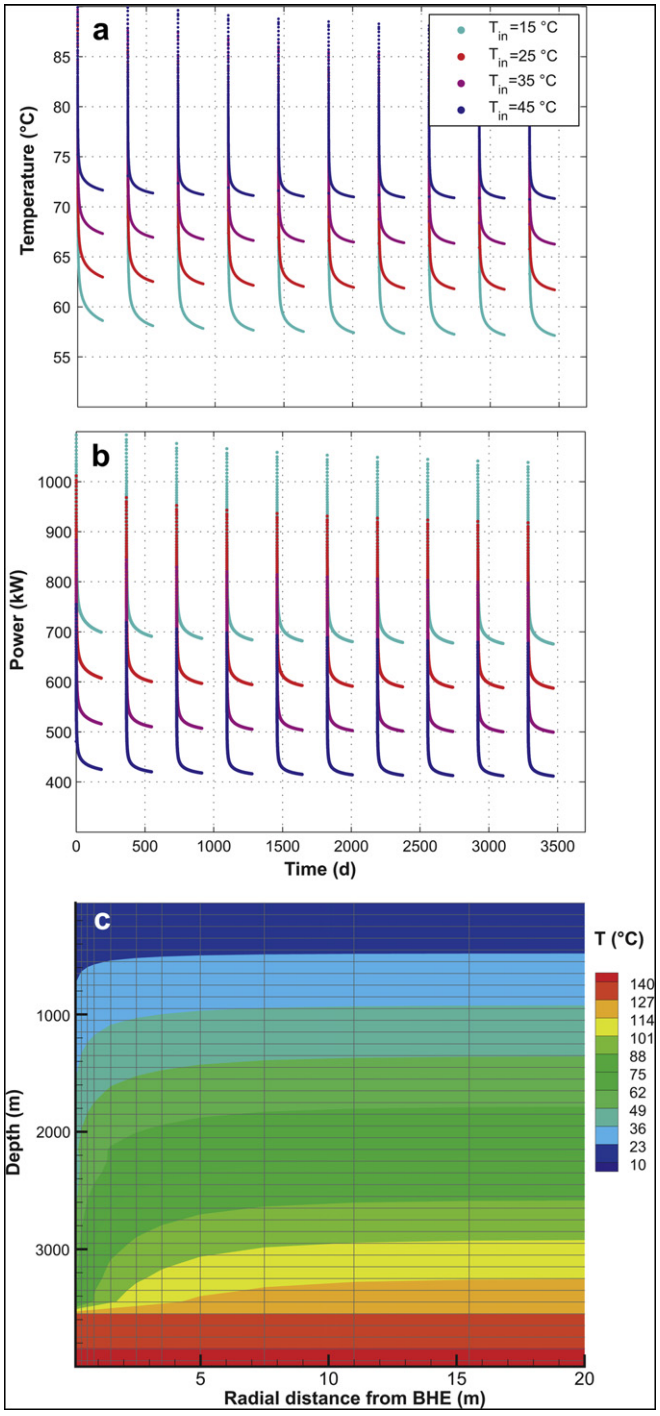

Fig. 10. Example for the behavior of a 3.6 km deep BHE. (a) Outlet temperatures for a biannual operation mode for ten years. The different colors indicate different inlet temperatures. (b) The associated power to be gained with the different temperature differences between outlet and inlet temperatures at a flow rate of 15 $m^3\ h^{-1}$. (c) The temperature field around the BHE after ten years of operation.

3.2. Comparison with data

Generally, monitoring data from BHE systems which include all necessary information on the different system, geological, and thermal properties are sparse. Here, we take advantage of an extensive data set available, coming from the deep BHE in Weggis, Switzerland. Fig. 9a shows its assemblage. During several years, inlet and outlet temperatures, as well as the pump rate were monitored [27]. Further necessary information was taken from Kohl et al. [28]. In Fig. 9b we plot a comparison for the time period from October 2002 to September 2003.

The grey line represents the model's inlet temperature, which was interpolated using the data (grey dots). The flow rate through the system is not constant as it varies from 3.3 to 6.1 $m^3\ h^{-1}$. There is a good agreement between the measured (black dots) and modeled outlet temperatures (black line).

3.3. Example for a deep BHE

As an example, we show a results from a study for a 3.6 km deep BHE in Northern Germany, for which an optimized operation mode was sought, in terms of a certain energy demand. Long term modeling, simulating the BHE for a decade or more, allows to determine if the system will come to a quasi steady-state condition. This means that the BHE runs in a sustainable mode. Fig. 10 shows outlet temperatures for different inlet temperatures (a), as well as the power which can be provided in this biannual operation mode (b). The heat carrier fluid is water at flow rate of 15 $m^3\ h^{-1}$. Temperatures do not decrease anymore in the course of the years, which means that the heat extraction and the heat supply by the surrounding rock will be in balance. The relating temperature field in this cylindrical model is shown in Fig. 10c), where the extent from the BHE of significant cooling can be visualized, which remains in this case less than 10 m. During the half year break, the ground temperatures recover, which yields this rather small value. For other operation modes, such as a continuous one, the radius with significant cooling is larger. Thus, due to the various parameters influencing the behavior of a deep BHE, numerical modeling which includes all the different processes is a prerequisite for a successful design.

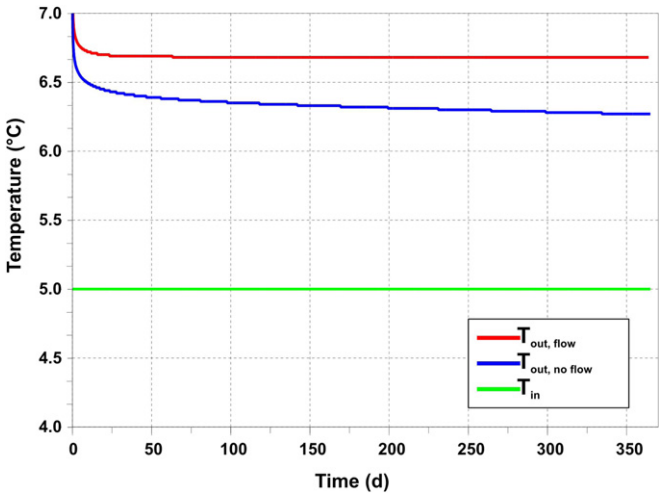

Fig. 11. The influence of groundwater flow on the outlet temperature of the modeled BHE.

3.4. Impact of groundwater flow

In order to study the influence of groundwater flow, we set up a 3-D model with a 100 m BHE with properties corresponding to the example given in the last section (Table 2). However, in this case we fix the inlet temperature at 5 °C, and the whole model domain is affected by groundwater flow at a Darcy velocity of 0.95×10^{-6} m s^{-1} (30 m a^{-1}). This allows quantifying the influence of groundwater flow in terms of the outlet temperature, when compared to the same model without groundwater flow. Fig. 11 shows that enough heat is advected by flow to reach a constant outlet temperature after 50 days. In the conductive model there is still no steady state behavior after one year. The resulting temperature field in both cases is plotted in Fig. 12. With groundwater flow present (Fig. 12b), the asymmetric temperature field is clearly visible.

In a next model run, we use the same BHE as shown in Table 2, but apply now a varying power profile, as shown in Table 4. Hence, it is possible to quantify approximately the performance gain for different ground water velocities. Fig. 13 shows the result for two years of operation. In Fig. 13a, the outlet temperatures for different ground water velocities are shown, the inlet temperature in the purely conductive case (no groundwater flow) is plotted as a reference. It becomes evident that even with the lowest groundwater velocity of 5.8×10^{-7} m s^{-1}, the outlet temperatures in the second year reach the same values as in the first year, thus the system is in steady-state conditions from the beginning. This does not hold for the conductive case, as seen from the outlet temperatures. In Fig. 13b, the performance gain for the different ground water velocities is plotted for the first year of operation, using the inlet temperature of the conductive case as a reference, which means that this temperature is considered as the inlet temperature for the different advective cases. This is of course an approximate approach, for a detailed study further simulations are necessary. Due to the non steady-state conditions in the purely conductive case and thus the temperature decrease in the following years, the performance gain will further increase. This example shows that it is worth taking a closer look at the hydrological conditions and performing numerical simulations. This ensures on the one hand to obtain a sustainable configuration, and on the other hand to save investment costs in terms of number and length of the BHEs.

4. An approximation for larger models

Although our approach avoids the fine discretization of the BHE assemblage, it is acceptable for only a few BHE in one model in terms of reasonable computing times. As explained above, this is due to numerical constraints such as the Courant criterion within the FD formulation of the BHE, which requires rather small time steps in order to account for the flow within the pipes.

However, often it is important to consider a whole field of BHEs which can consist of several tenths or even hundreds of single BHEs. In this case an explicit calculation of the fluid flow within the pipes becomes too time consuming. Here, we developed an approximation which transfers heating and cooling loads as in Table 3 into an effective heat generation along the BHEs. In principle, this approximation is based on the SHEMAT code itself, but with the possibilities to easily consider varying power profiles with arbitrary time intervals, and to position the BHEs anywhere in a 3-D model. In this case, no inlet or outlet temperatures are calculated, but it is possible to analyze the temperatures around a BHE field, whose type, coaxial or double-U shaped, is arbitrary. This is particular interesting in the presence of groundwater flow, when cold or warm plumes are carried away by advection.

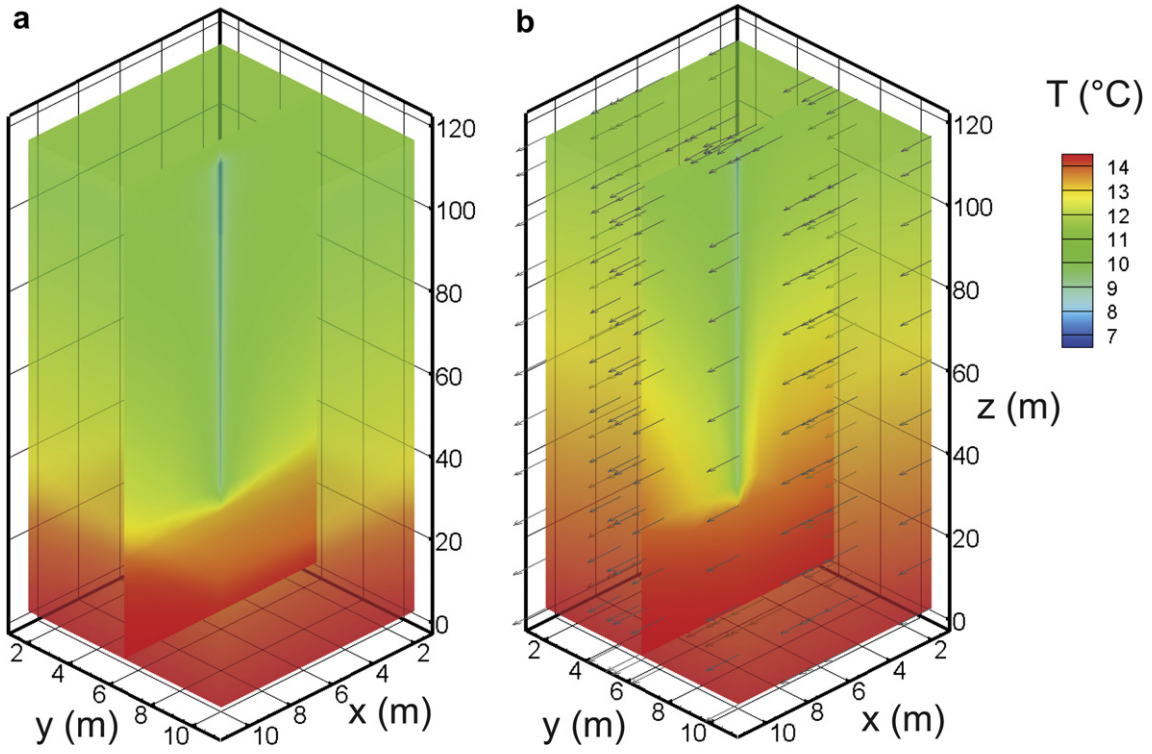

Fig. 12. Temperature field of the synthetic model in order to study the influence of groundwater flow (a) Conductive model (b) Model including flow at 0.95×10^{-6} m s^{-1} (30 m per year).

Table 4
Monthly power profile (kW) used for the demonstration of the impact of groundwater flow. The BHE is assumed to run constantly at these values. The total annual energy extracted from the underground is 12 MWh.

January	February	March	April	May	June	July	August	September	October	November	December
2.92	2.5	2.08	1.67	0.0	0.0	0.0	0.0	0.0	2.29	2.5	2.5

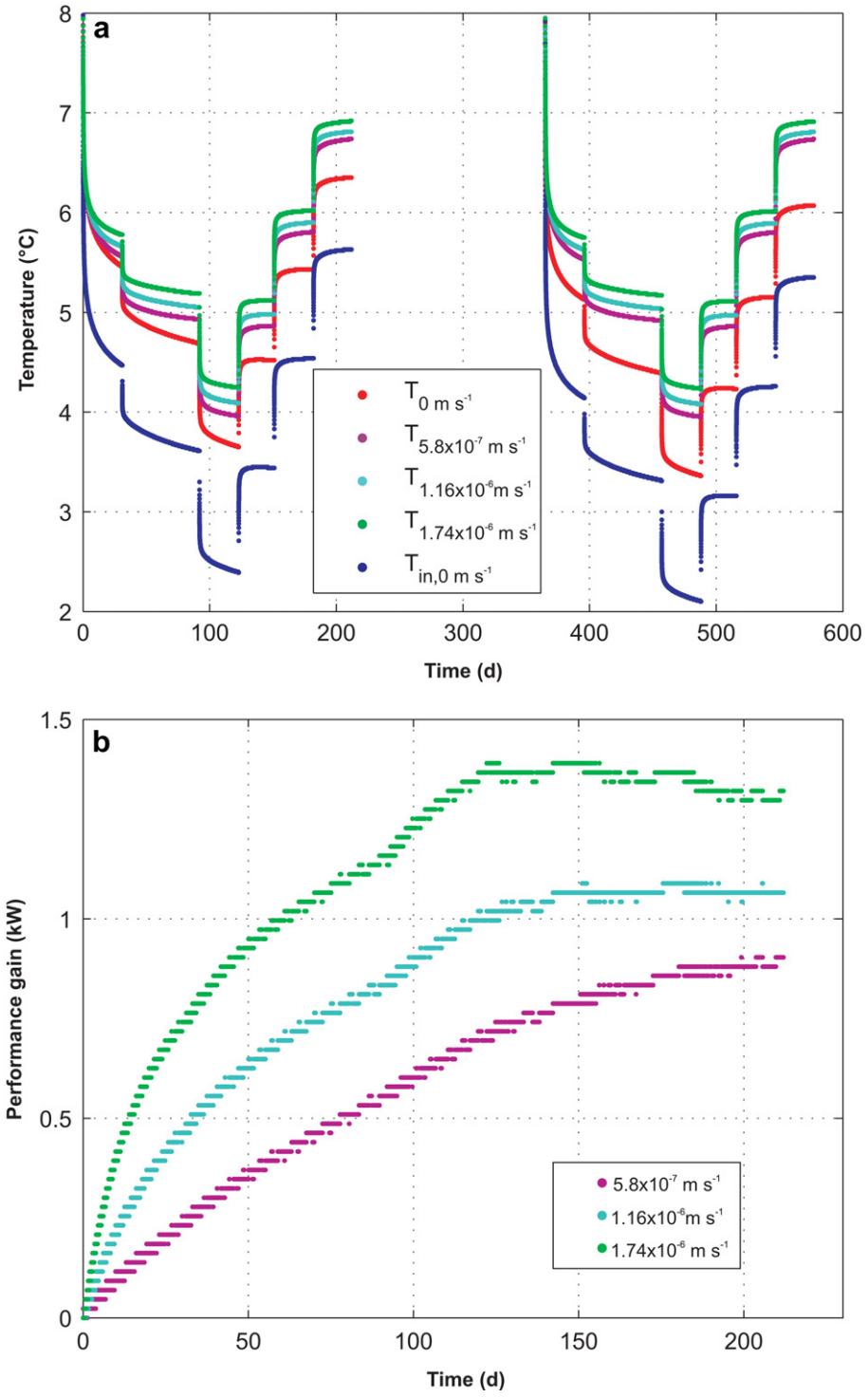

Fig. 13. Behavior of a BHE with respect to different ground water velocities. The associated power profile is shown in Table 4. (a) Outlet temperatures for different ground water velocities and inlet temperature for the conductive case. (b) Performance gain when considering the inlet temperature from the conductive case as the inlet temperature for the different advective cases.

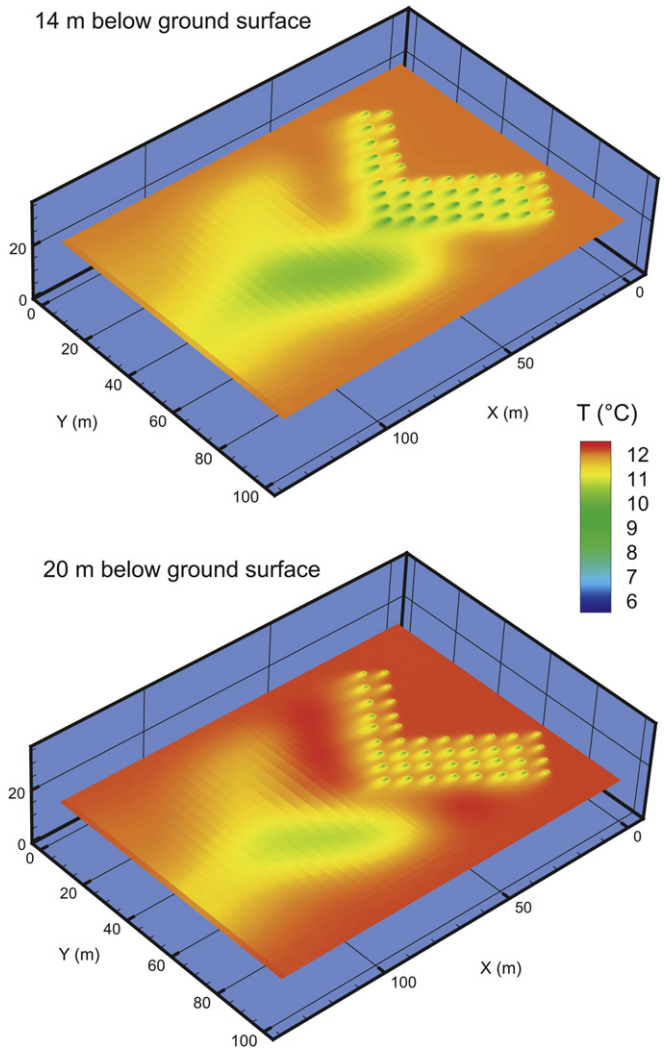

Fig. 14. Temperature field at two different depths around an BHE field comprising 42 double U-shaped BHEs after 15 years simulation time.

Regulating authorities consider this as a major issue when dealing with permissions for BHEs, particularly in densely developed areas [29].

Fig. 14 shows an example of an L-shaped BHE field consisting of 42 BHEs, each 30 m deep. The simulation time is 15 years, and the aquifer is situated between 11 and 28 m below ground surface, with a groundwater flow velocity of 1.19×10^{-6} m s^{-1} (37.5 m per year). In 20 m depth, a cold plume becomes clearly visible, resulting from the cooling around the BHEs from the preceding winter.

5. Conclusion

We present the coupling of a finite difference formulation of BHE with the general code for heat and transport modeling SHEMAT. In principle, this approach can be used in any finite difference or finite element code. The connection between the BHE model and SHEMAT on different scales is realized by introducing an apparent heat generation in the latter one. Thus it is possible to consider an arbitrary, heterogeneous geologic model, as well as the influence of groundwater flow in the surroundings of one or multiple borehole heat exchangers. The model is validated against existing models and field data, showing a satisfactory agreement.

Our approach is especially suitable for the modeling of deep BHE with varying pipe assemblages. For these kinds of BHEs, the complexity of the installation, the coupling with the underground, and various different operation modes require a thorough simulation. It must account for all technical, geological, and thermophysical properties; our method fulfills these requirements.

Generally, we can state that CPU-times are decreased by more than an order of magnitude, when comparing the method presented here with a pure numerical model using the code SHEMAT alone. Due to this improvement, it is possible to study the system's long term behavior, i.e. over the course of several years and decades. These time periods are often necessary for a reliable assessment and thus a sustainable design of a BHE system. This is especially the case for more complicated situations, in terms of heterogeneity and advective conditions, where a more simple design tool is possibly not applicable anymore.

For shallow BHE fields, we developed a slimmed-down version of the method presented, based on the original SHEMAT code, but with more options regarding the operation modes. It is suitable for studying the propagation of cold and warm plumes in the surrounding subsurface.

From the results of our study, and after gaining experience working with BHE simulations, we propose a general, stepwise procedure when designing shallow BHE systems:

1. Application of an analytical and fast program such as EED or EWS for the field design.
2. If geology is complicated, or groundwater flow is present, the simulation of one or a few BHE with a modeling tool as presented here.
3. Extrapolation of results in step 2 with those from step 1 for a comprehensive view on the performance prediction of the system.
4. Particular for large BHE fields: study of the influence of the BHE system on the temperature field in the manner as presented in Section 4.

Appendix A. Thermal resistances of a borehole heat-exchanger

For a cylinder, the heat flow rate $\dot{Q}$, using Fourier's law is;

$$\dot{Q} = -\lambda A \frac{\mathrm{d}T}{\mathrm{d}r} \tag{A.1}$$

with surface area $A = 2\pi r dz$, dz and r respectively the length and radius of the pipe and λ the thermal conductivity.

Generally for n cylinders, we have

$$\dot{Q} = \frac{T_{n+1} - T_1}{R} \tag{A.2}$$

with R the overall thermal resistance of n cylinder [14].

Appendix A.1. Thermal resistance of inner cylinder R'_{inner}

The total thermal resistance in case of flow inside and outside the cylinders is;

$$R'_{inner} = R_{inner} dz = R'_e = R'_{conv(inner)} + R'_{cond} + R'_{conv(inner')} \tag{A.3}$$

The total conductive thermal resistance of n conductive cylinders inside each other is:

$$R'_{cond} = \sum_{i}^{n} \frac{1}{2\pi\lambda_i} \ln\left(\frac{r_{inner'}}{r_{inner}}\right) \tag{A.4}$$

r_{inner} and $r_{inner'}$ are described in Fig. 4

If fluid moves inside or outside the inner cylinder, the convective thermal resistance is given by:

$$R'_{conv(inner)} = \frac{1}{h_{inner} A_{inner}} \tag{A.5}$$

$$R'_{conv(inner')} = \frac{1}{h_{inner'} A_{inner'}} \tag{A.6}$$

with $h_{inner} = Nu\lambda_w/(2r_{inner})$ and $h_{inner'} = Nu\lambda_w/(2r_{inner'})$ the heat transfer coefficient to the inside or outside of the inner cylinder, λ_w the thermal conductivity of water, and $A_{inner} = 2\pi r_{inner} dz$, $A_{inner'} = 2\pi r_{inner'}$ the surface area and Nu Nusselt number. The heat transfer coefficient is depending on the geometry and the properties of the flow.

In thermodynamics the Nusselt number Nu is depending on the flow type – turbulent or laminar. We can use the Reynolds number Re to distinguish between these to types.

- In case of turbulent; $Re > 2300$ then $Nu = 0.023\,\mathrm{Re}^{0.8} Pr^{0.3}$ (Dittus–Boelter equation) with Pr the Prandtl number.
- In case of laminar; $Re < 2300$ then $Nu = 3.66$

with Re Reynolds number for the inner pipe defined as;

$$\mathrm{Re}_{inner} = \frac{2 r_{inner} F_w}{\pi \nu_w r_{inner}^2} \tag{A.7}$$

with ν_w the kinematic viscosity, $r_{inner}, r_{outer}, r_{inner'}$ defined in Fig. 4 and F_w the flow rate.

The Prandl number is

$$Pr = \nu_w C_w / \lambda_w \tag{A.8}$$

Appendix A.2. Thermal resistance outer cylinder R'_{outer}

The outer thermal resistance R_{outer} is divided into two parts, one associated with the convective resistance and one due to conductive resistance. This resistance is assumed to be in steady state because of the relatively small volume and diffusivity time, compared to the rocks surrounding the pipe. The above description is only valid if we assume a fast steady state behavior. This is the case for small thickness's and high thermal conductivity of the pipe wall. For borehole heat-exchangers this is commonly used as a good approximation.

$$R'_{outer} = R_{outer} dz = R'_{b,conv} + R'_{b,cond} \tag{A.9}$$

If fluid moves inside the outer cylinder, the convective thermal resistance is given by;

$$R'_{b,conv} = \frac{1}{h_{outer} A_{outer}} \tag{A.10}$$

The total conductive thermal resistance of n conductive cylinders inside each other is:

$$R'_{b,cond} = \sum_{i}^{n} \frac{1}{2\pi\lambda_i} \ln\left(\frac{r_i}{r_{i+1}}\right) \tag{A.11}$$

with $h_{outer} = Nu\lambda_w/(2r_{outer})$ the heat transfer coefficient to the outer cylinder, λ_w the thermal conductivity of water, and $A_{outer} = 2\pi r_{outer}$, the surface area and Nu Nusselt number.

The Nusselt number Nu is depending on the flow type - turbulent or laminar, and can be determined using Section A.1 and with Re Reynolds for outer pipe defined as:

$$Re_{outer} = \frac{2 r_{outer} F_w}{\pi \nu_w \left(r_{outer}^2 - r_{inner'}^2\right)} \tag{A.12}$$

with ν_w the kinematic viscosity, $r_{inner}, r_{outer}, r_{inner'}$ defined in Fig. 4 and F_w the flow rate.

Appendix A.3. Thermal resistance of the water in the pipes are R_u and R_d

R_u and R_d are the resistances of water in respectively the inner and outer pipe

$$R_d = \frac{dz}{\lambda_w \pi \left(r_{outer}^2 - r_{inner'}^2\right)} \tag{A.13}$$

$$R_u = \frac{dz}{\lambda_w \pi r_{inner}^2} \tag{A.14}$$

Appendix A.4. Thermal resistances for double-U shaped BHE after [23]

The thermal borehole resistance R_b for a double-U shaped BHE is adapted from Hellström (1991). The internal thermal resistance R_a describing the coupling between the upward and downward flow in the pipes is:

$$R_a = \frac{1}{\pi \cdot \lambda_{gr}} \left[\ln\left(\frac{\sqrt{2} \cdot b \cdot r_b}{r_{pipe}}\right) - \frac{1}{2} \cdot \ln\left(\frac{2 \cdot b \cdot r_b}{r_{pipe}}\right) - \frac{1}{2} \cdot \sigma \ln\left(\frac{1 - b^4}{1 + b^4}\right) \right] + \frac{1}{2 \cdot \pi \cdot r_{pipe} \cdot h} + R_{pipe} \tag{A.15}$$

with

$$R_{pipe} = \frac{1}{2 \cdot \pi \cdot \lambda_{gr}} \cdot \ln\left(\frac{r_{pipe'}}{r_{pipe}}\right) \tag{A.16}$$

and $b = Bu/(2 \cdot r_b)$ which describes the position of the pipes and $\sigma = (\lambda_{gr} - \lambda_r)/(\lambda_{gr} + \lambda_r)$ the conductivity parameter.

The borehole thermal resistance is derived from the line-source approximation with a first order multipole correction:

$$R_b = \frac{1}{8\cdot\pi\cdot\lambda_{gr}}\cdot\left[\beta + \ln\left(\frac{r_b}{r_{pipe}}\right) + \ln\left(\frac{r_b}{Bu}\right) + \sigma\cdot\ln\left(\frac{r_b^4}{r_b^4 - \frac{Bu^4}{16}}\right) - \frac{\frac{r_{pipe}^2}{Bu^2}\left[1 - \sigma\cdot\frac{\frac{1}{4}Bu^4}{\left(r_b^4 - \frac{Bu^4}{16}\right)}\right]^2}{\left\{\frac{1+\beta}{1-\beta} + \frac{r_{pipe}^2}{Bu^2}\left[1 + \sigma\cdot\frac{Bu^4\cdot r_b^4}{\left(r_b^4 - \frac{Bu^4}{16}\right)^2}\right]\right\}}\right] \quad \text{(A.17)}$$

where

$$\beta = \lambda_{gr}\cdot\left[\frac{1}{r_{pipe}\cdot h} + \frac{1}{\lambda_{pipe}}\cdot\ln\frac{r_{pipe'}}{r_{pipe}}\right] \quad \text{(A.18)}$$

with the heat transfer coefficient $h = Nu\lambda_w/(2\cdot r_{pipe})$.

References

[1] Florides G, Kalogirou S. Ground heat exchangers—a review of systems, models and applications. Renewable Energy 2007;32(15):2461–78. doi:10.1016/j.renene.2006.12.014.

[2] Hellström G, Sanner B. EED Earth Energy Designer, User Manual. version 3.0 Available at: http://www.buildingphysics.com/earth1.htm; 2008.

[3] Huber A. Software Manual of the program EWS. Version 4.7. Zurich, Switzerland: Huber Energietechnik AG Ingenieur- und Planungsbüro; 2011.

[4] Eskilson P. Thermal analysis of heat extraction boreholes. Ph.D. thesis; University of Lund, Department of Mathematical Physics. Lund, Sweden; 1987.

[5] Diao N, Li Q, Fang Z. Heat transfer in ground heat exchangers with groundwater advection. International Journal of Thermal Sciences 2004;46:1203–11.

[6] Sutton M, Nutter D, Couvillion R. A ground resistance for vertical bore heat exchangers with groundwater flow. Journal of Energy Resources Technology 2003;125:183–9.

[7] Muraya NK. Numerical modeling of the transient thermal interference of vertical U-tube heat exchangers. Ph.D. thesis; Texas A&M University; 1994.

[8] Zeng H, Diao N, Fang Z. Heat transfer analysis of boreholes in vertical ground heat exchangers. International Journal of Heat and Mass Transfer 2003;46(23):4467–81. doi:10.1016/S0017-9310(03)00270-9.

[9] Signorelli S. Geoscientific Investigations for the use of shallow low-enthalpy systems. ETH Dissertation 15519 Swiss Federal Institute of Technology, Zürich; 2004.

[10] Li Z, Zheng M. Development of a numerical model for the simulation of vertical U-tube ground heat exchangers. Applied Thermal Engineering 2009;29(5–6):920–4. doi:10.1016/j.applthermaleng.2008.04.024.

[11] Lamarche L, Kajl S, Beauchamp B. A review of methods to evaluate borehole thermal resistances in geothermal heat-pump systems. Geothermics 2010;39(2):187–200.

[12] Chiasson A, Yavuzturk C, Nydahl J. Simulation model for ground loop heat exchangers. ASHRAE Transactions 2009;115(2).

[13] De Carli M, Tonon M, Zarrella A, Zecchin R. A computational capacity resistance model (CaRM) for vertical ground-coupled heat exchangers. Renewable Energy 2010;35(7):1537–50.

[14] Çengel Y, Turner R, Cimbala JM. Fundamentals of Thermal-Fluid Sciences. 3rd ed. New York: McGraw-Hill, ISBN 978-0-07-352925-7; 2008. p. 672, 938.

[15] Dijkshoorn L, Wagner R. Performance simulations for a deep borehole heat exchanger in Aachen. In: International workshop on "New and Classical Applications of Heat Flow Studies in Aachen, October 4–7; 2004.

[16] Speer S. Design calculations for optimising of a deep borehole heat-exchanger. Master's thesis; RWTH Aachen University; 2005.

[17] Dijkshoorn L. Designing a new effective finite difference formulation for borehole heat exchangers. 67. Jahrestagung der Deutschen Geophysikalischen Gesellschaft, 26–29. März, Aachen. Abstracts, S 125.; 2007.

[18] Dijkshoorn L. The Earth as Energy Stock - Natural and enhanced behavior of thermal resistances, heat storage capacity and heat flow in the Earth and their relevance to the geothermal power of a deep coaxial borehole heat exchanger in the Eifel-Maas region; Ph.D. thesis, RWTH Aachen University, in preparation.

[19] Clauser C, editor. Numerical Simulation of Reactive Flow in Hot Aquifers. SHEMAT and PROCESSING SHEMAT. New York: Springer; 2003.

[20] Bear J. Dynamics of Fluids in Porous Media. New York: Dover; 1972.

[21] Ferguson G. Heterogeneity and thermal modeling of ground water. Ground Water 2007;45(4):485–90.

[22] Molina-Giraldo N, Bayer P, Blum P. Evaluating the influence of thermal dispersion on temperature plumes from geothermal systems using analytical solutions. International Journal of Thermal Sciences 2011;50(7):1223–31.

[23] Hellström G. Ground heat Storage. Thermal Analyses of Duct Storage Systems. Ph.D. thesis; Theory. Dep. Of Mathematical Physics, University of Lund; 1991.

[24] Wylie EB, Streeter VL. Fluid transients. McGraw-Hill International Book Co; 1978. Republished with minor corrections by FEB Press, Ann Arbor, NY, 1983.

[25] Signorelli S, Kohl T. Validieren des Programms EWS und Optimieren der Erdwärmesondenlänge. Tech. Rep. Swiss Federal Office of Energy; 2002

[26] Kohl T, Hopkirk RJ. FRACTure – a simulation code for forced fluid flow and transport in fractured, porous rock. Geothermics 1995;24(3):333–43.

[27] Eugster W, Füglister H. Tiefe Erdwärmesonde Weggis, Messkampagne zur Dokumentierung der neuen Einflüsse beim Ausbau der Abnehmerleistung. Tech. Rep. Swiss Federal Office of Energy; 2003.

[28] Kohl T, Brenni R, Eugster W. System performance of a deep borehole heat exchanger. Geothermics 2002;31:687–708.

[29] Haehnlein S, Bayer P, Blum P. International legal status of the use of shallow geothermal energy. Renewable and Sustainable Energy Reviews 2010;14(9):2611–25.

[30] Eugster W, Füglister H. Tiefe Erdwärmesonde Weggis 1. Schlussbericht zu Händen des Bundesamtes für Energie, Bern, und des Projekt- und Studienfonds der Elektrizitätswirtschaft, Olten. Tech. Rep.. Swiss Federal Office of Energy; 1997